Reverse-time migration by fan filtering plus wavefield decomposition

Sang Yong Suh, KIGAM and Jun Cai, TGS-NOPEC*

SUMMARY

The conventional zero-lag crosscorrealtion imaging condition of reverse-time migration is subject to strong migration artifacts. This paper studies wavefield decomposition method under relatively complex subsurface. Although the method greatly suppresses the internal reflection noise, it is subject to residual noise. To suppress the residual noise, we apply a fan filtering on each wave field snapshot in space domain. The filtered wavefields are further decomposed into downgoing and upgoing components and into leftgoing and rightgoing components. The decomposition is carried on F-K domain.

INTRODUCTION

Reverse-time migration propagates wavefields in time through the use of two-way wave equation (Baysal et al., 1984; Whitmore, 1983). It correctly handles both multi-arrivals and phase changes. It's main advantage over one-way wave equation techniques is that it has no dip limitation. Thus, reverse-time migration enables imaging of very complex subsurface. Two-way migration methods require significantly greater computational resources than one-way migration methods. However, as a consequence of improved computer hardware, there has been recent interest in reverse-time migration (Bednar et al., 2003; Yoon et al., 2003).

Prestack reverse-time migration is accomplished in two steps. First, a shot signature at surface is propagated forward in time using a two-way wave equation and saved on a disk file. Second, the recorded surface wavefield is time-reversed and backward propagated using the same wave equation. The time-reversed receiver wavefield is then time unreversed to produce full receiver wavefield. The migration image is computed by zero-lag crosscorreation of the source and receiver wavefields.

The imaging condition, however, is subject to image artifacts. Unwanted crosscorrelation of head waves, diving waves, and backscattered waves appear as image artifacts. Various methods are since proposed to suppress these noise. Mulder and Plessix (2003) used using a low cut filtering in space domain. Valenciano and Biondi (2002) proposed a deconvolution imaging condition which is based on inverse theory. Chang and McMechan(1986, 1990) suggested ray-traced imaging condition, in which source wavefield after the first arrival is limited to some fixed time duration. This automatically excludes all but postcritical reflections from the source wavefield. Fletcher et al. (2006) modified the wave equation to include a directional damping term in areas of the velocity model where unwanted reflections occur.

Yoon and Marfurt (2006) suggested using Poynting vectors which will determine the direction of wavefield propagation and to decompose into upgoing and downgoing waves. Liu et al. (2007) decomposed the full wavefields into their one-way components, and applied the imaging condition to the appropriate combinations of the wavefield components.

In this paper, we study wavefield decomposition method by migrating a synthetic seismic data over a complex subsurface. Although the wavefield decomposition method greatly suppresses the internal reflection noise, it is subject to significant residual reverse-time noise. The residual noise is analyzed. To suppress the residual noise, we apply a fan filtering on each wave field snapshot in space domain. The filtered wavefields are further decomposed into downgoing and upgoing components and into leftgoing and rightgoing components. The decomposition is carried on F-K domain. Different imaging condition is used depending on the dip of the target structure

THEORY

The conventional migration image, $I(\mathbf{x})$, is computed by zero-lag crosscorreation of the source and receiver wavefields as

$$I(\mathbf{x}) = \int_0^{t_{max}} S(t,\mathbf{x})R(t,\mathbf{x})dt, \tag{1}$$

where $S(t,\mathbf{x})$ is the source wavefield, $R(t,\mathbf{x})$ is the time-unreversed receiver wavefield, and t_{max} is the maximum recording time.

In reverse-time migration, the source wavefield contain wave components propagating in all directions. Referencing to the z direction, the wavefield can be decomposed into downgoing and upgoing components as

$$S(t,\mathbf{x}) = S_{z+}(t,\mathbf{x}) + S_{z-}(t,\mathbf{x}), \tag{2}$$

where $S_{z+}(t,\mathbf{x})$ and $S_{z-}(t,\mathbf{x})$ are the downgoing and upgoing source wave component, respectively. The receiver wavefield can be decomposed in a similar way as

$$R(t,\mathbf{x}) = R_{z+}(t,\mathbf{x}) + R_{z-}(t,\mathbf{x}), \tag{3}$$

where $R_{z+}(t,\mathbf{x})$ and $R_{z-}(t,\mathbf{x})$ are the downgoing and upgoing receiver wavefield component, respectively. Substituting equation (2) and (3) to equation (1), we get

$$\begin{aligned} I(\mathbf{x}) = &\int_0^{t_{max}} S_{z+}(t,\mathbf{x})R_{z-}(t,\mathbf{x})dt + \int_0^{t_{max}} S_{z-}(t,\mathbf{x})R_{z+}(t,\mathbf{x})dt \\ &+ \int_0^{t_{max}} S_{z+}(t,\mathbf{x})R_{z+}(t,\mathbf{x})dt + \int_0^{t_{max}} S_{z-}(t,\mathbf{x})R_{z-}(t,\mathbf{x})dt \end{aligned}$$

Liu et al. (2007) showed that the first term is equivalent to those in the one-way wave equation migration. The second term is caused by a upgoing source wavefield striking a horizontal interface from bottom and reflected downward. Therefore, the first two terms are signal. On the other hand, the third and fourth terms are noise. To eliminate the noise, they choose an imaging condition to include the first two terms only. We shall name it *vertical wave imaging condition* because vertically propagating waves are used. This is useful for imaging mild dip structure. Similar decomposition can be made on horizontally propagating waves to give *horizontal wave imaging condition*, which will be useful for imaging steep dip structure.

Figure 1 shows reverse-time migration images of BP 2004 model seismic data using the vertical wave imaging condition. The image shows good resolution for the horizontal layers and at the salt top. However, there are strong low frequency noise near the salt flanks.

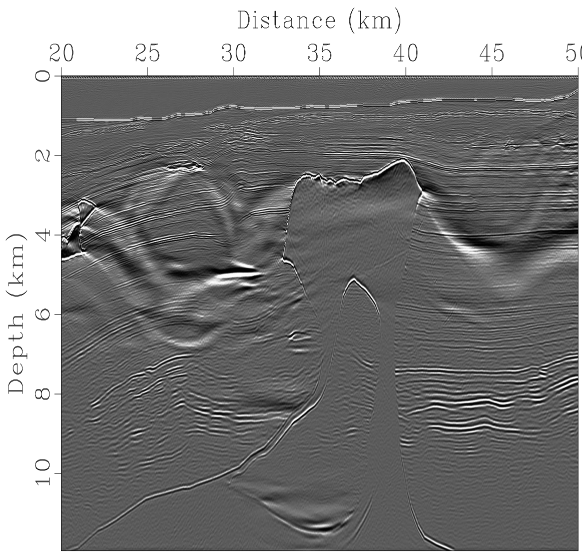

Figure 1: Reverse-time migration of BP 2004 model seismic data using vertical wave imaging condition.

Figure 2(a) shows source wavefield excited at $x = 30km$ in time-depth domain. The left panel is full source wavefield. The center panel is downgoing component. The right panel is upgoing component. This demonstrates how we can decompose a wavefield into downgoing and upgoing components. The idea is to represent the wavefield in time-depth domain, apply 2D FFT, zero-out either odd or even quadrant, and take inverse transform.

Starting from the origin (upper-left corner) of the left panel, we notice an event whose depth is increasing as time increases. This is a downgoing wave. And it is the first arrival. At depth $5km$ and time $2.5s$, there is a weak reflection. (The plot gain is too small to reveal this. However, it is amplified on the right panel.) And at depth $5km$ and time $3.8s$, there is a strong hyperbolic event. This is not a reflection, and is the reason of the strong low frequency noise found at Figure 1. There is also a group of hyperbolic events at time $5s$ and depth 6-8 km. These hyperbolas are not removed by the wavefield decomposition.

Figure 2(b) shows the source wavefield snapshot at time $3.8s$ in depth(z)-distance(x) domain. From the left panel of the figure we try to locate an event at $z = 5km$ and $x = 30km$ corresponding to the strong hyperbola peak in Figure 2(a). And we confirm that there is an event. The shape of the wavefront suggests that it is propagating horizontally leftward. Further snapshot movie analysis shows that the event is a scattering wave originated from the salt flank at $x = 32.5km, z = 4.6km$. As the scattered wave arrives near $x = 30km, z = 5km$, the wave path becomes horizontal due to gradual increase of the velocity. Anyway, the low freqnecy noise on Figure 1 is due to the horizontally propagating waves which are not separable into upgoing and downgoing waves. To remove this noise, we apply a fan filtering. The center panel of Figure2(b) shows vertically propagating wavefields passing 60 degree or less from vertical and linearly tapering out up to 75 degrees from vertical. The right panel shows horizontally propagating wavefields passing 60 degree or less from horizontal and linearly tapering out up to 75 degrees from horizontal. This suggests that the fan filtering combined with the wavefield decomposition could remove almost all artifacts in reverse-time migration.

Figure 3(a) shows the reverse-time migration images of one shot gather. The source location is $x = 30km$. The image on left panel is using conventional zero-lag corsscorrelation. The image on center panel is using the vertical wave imaging condition. The image on right panel is computed using a fan filtering and then imaged by the vertical wave imaging condition.

Figure 3(b) shows the reverse-time migration of BP 2004 model seismic data by fan filtering plus wavefield decomposition. The left panel used vertical wave imaging condition. The center panel used horizontal wave imaging condition. As expected earlier, the vertical wave imaging condition is useful to map the horizontal layers, while the horizontal wave imaging condition is good for mapping vertical boundaries. The plot gains are different between these two panels. The right panel is the arithmetic sum of the two images. Comparing this with Figure 1, we find all the low frequency noises are successfully removed.

DISCUSSION

Current method carries wavefield decomposition in time-space domain. This means that the saved wavefield snapshots must be transposed in time-fast order. Because the volume of snapshots is generally much larger than CPU memory size, a disk-aided matrix transpose must be used which is very time consuming. Experience shows that the run time of this fan filtering plus wavefield decomposition method is at least six times longer than the conventional zero-lag crosscorrelation imaging. Also, the amount of disk space required is doubled because the receiver wavefield has to be saved as well as the source wavefield.

ACKNOWLEDGEMENTS

We thank Dr. Zhiming Li and Dr. Bin Wang of TGS-NOPEC for their advices and encourangements on wavefield decomposition research. We thank KIGAM and TGS-NOPEC for the permission to publish this paper. We also thank BP and Mr. Frederic Billette for providing BP 2004 model seismic data.

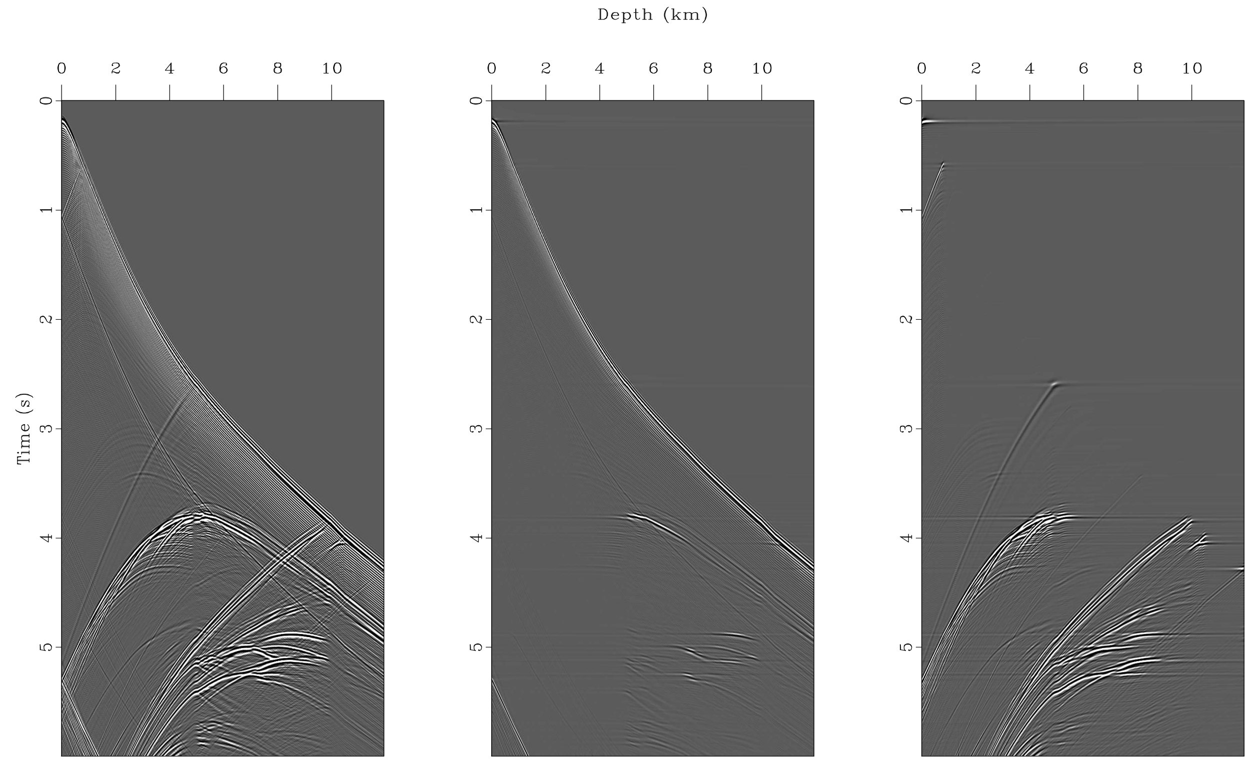

(a)

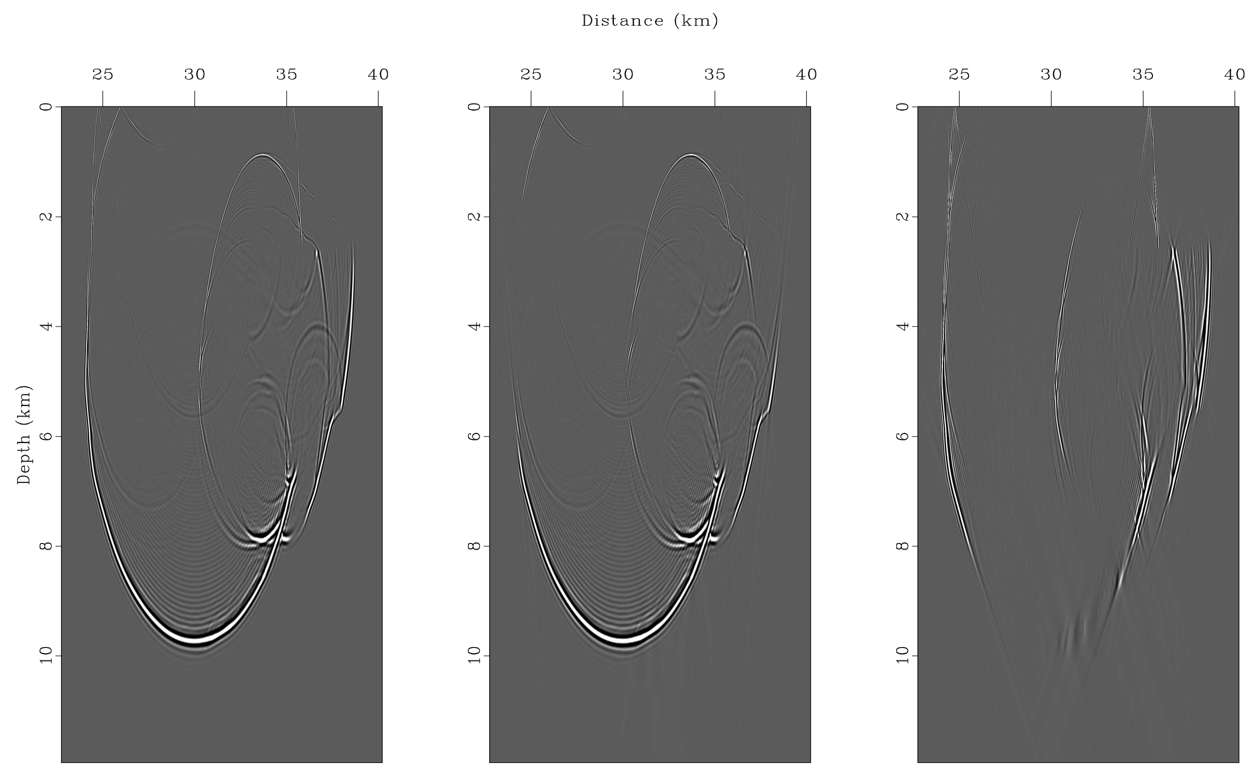

(b)

Figure 2: (a): Wavefield decomposition in time-depth domain: left) source wavefield excited at $x = 30km$; center) downgoing component; right) upgoing component. (b): Source wavefields excited at $x = 30km$ in $z-x$ domain: left) source wavefield snapshot at $t = 3.8s$; center) vertical wave enhanced; right) horizontal wave enhanced.

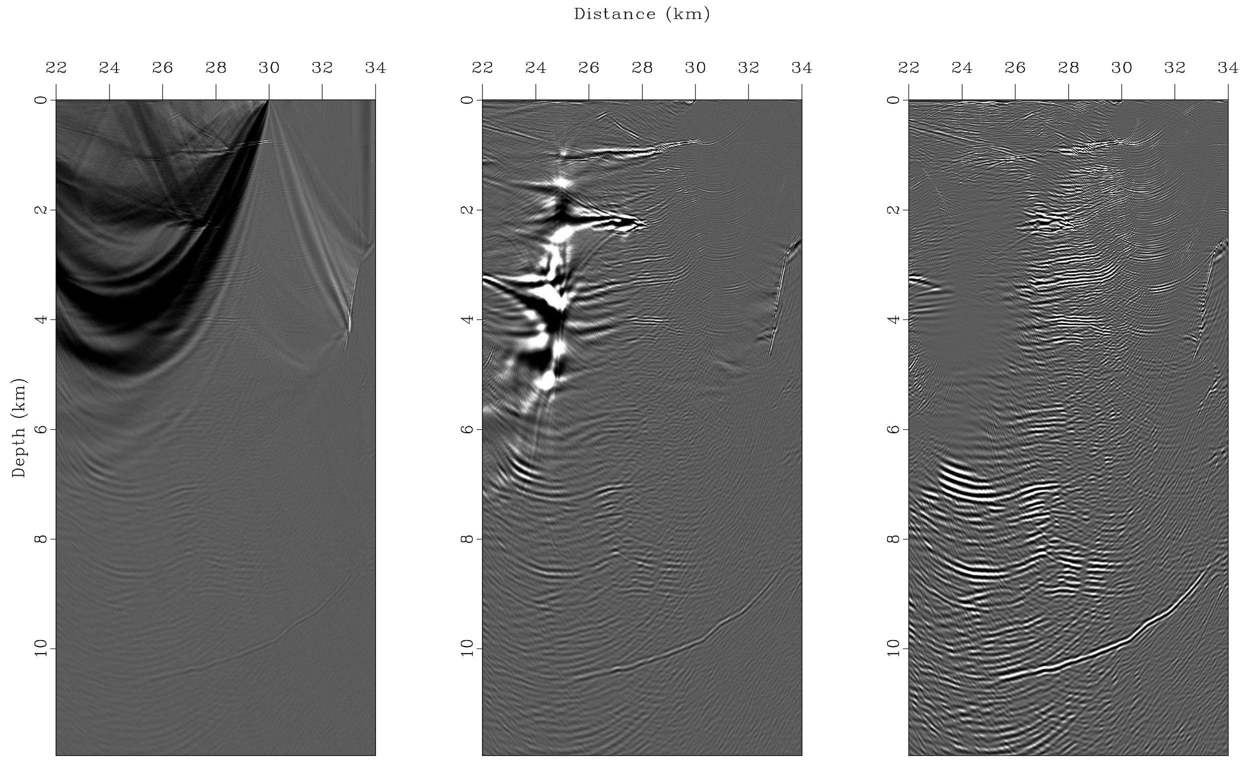

(a)

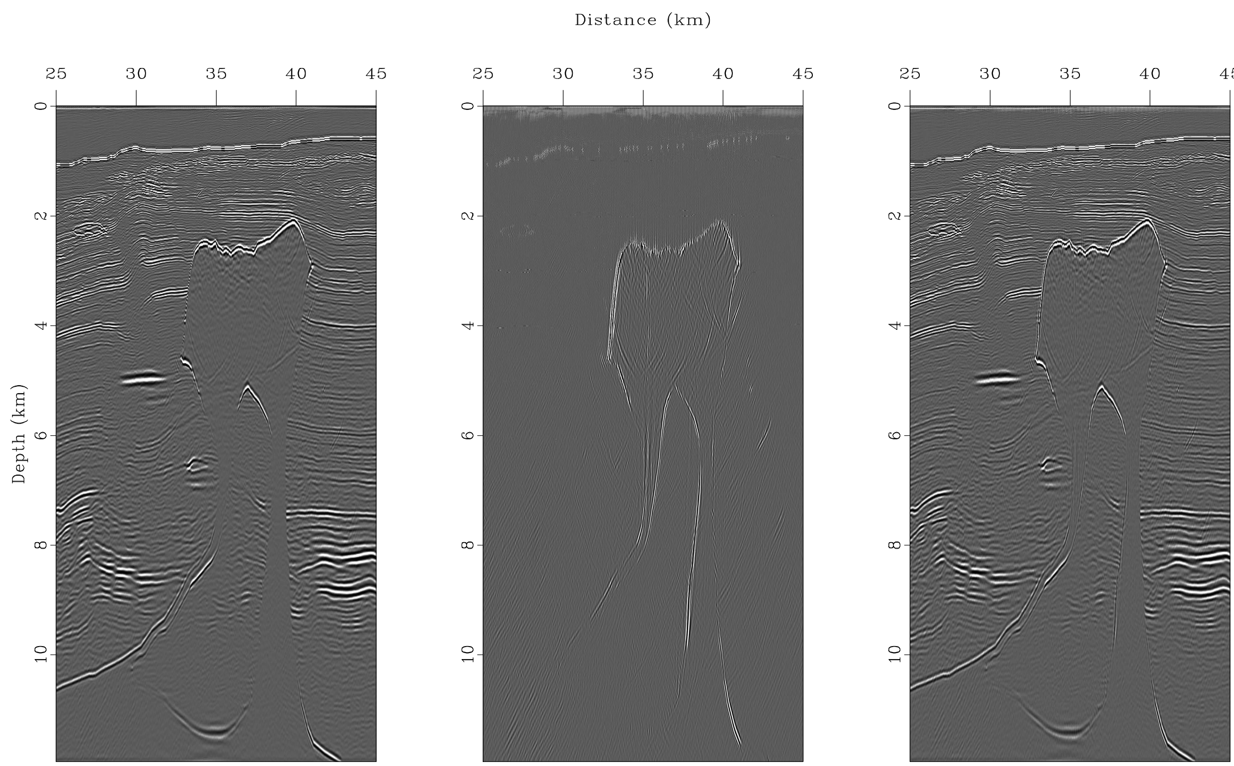

(b)

Figure 3: (a): Reverse-time migration of a shot at $x = 30km$: left) using conventioal zero-lag crosscorrelation; center) using vertical wave imaging condition; right) fan filtering plus vertical wave imaging condition. (b) Reverse-time migration of BP 2004 model seismic data by fan filtering plus wavefield decomposition: left) using fan filtering plus vertical wave imaging condition; center) using fan filtering plus horizontal wave imaging condition; right) sum of the two.

EDITED REFERENCES

Note: This reference list is a copy-edited version of the reference list submitted by the author. Reference lists for the 2009 SEG Technical Program Expanded Abstracts have been copy edited so that references provided with the online metadata for each paper will achieve a high degree of linking to cited sources that appear on the Web.

REFERENCES

Baysal, E., D. D. Kosloff, and J. W. C. Sherwood, 1984, Reverse-time migration: Geophysics, **48**, 1514–1524.

Bednar, J. B., J. Stein, K. Yoon, and C. Shin, 2003, An up and down talk in the two-way talk: 73rd Annual International Meeting, SEG, Expanded Abstracts, 877–880.

Chang, W. F., and G. A. McMechan, 1986, Reverse-time migration of offset vertical seismic profiling data using the excitation-time imaging condition: Geophysics, **51**, 67–84.

———, 1990, 3D acoustic prestack reverse-time migration: Geophysical Prospecting, **38**, 737–756.

Fletcher, B. B., P. J. Fowler, P. Kitchenside, and U. Albertin, 2006, Suppressing unwanted internal reflections in prestack reverse-time migration: Geophysics, **71**, no. 6, E79–E82.

Lin, F., G. Zhang, S. A. Morton, and J. P. Leveille, 2007, Reverse-time migration using one-way wavefield imaging condition: 77th Annual International Meeting, SEG, Expanded Abstracts, 2170–2174.

Mulder, W., and R. Plessix, 2003, One-way and two-way wave-equation migration: 73rd Annual International Meeting, SEG, Expanded Abstracts, 881–884.

Valenciano, A. A., and B. Biondi, 2002, Deconvolution imaging condition for reverse-time migration: Stanford Exploration Project, Report 112, 131–137.

Whitmore, D. N., 1983, Iterative depth imaging by back time propagation: 53rd Annual International Meeting, SEG, Expanded Abstracts, 382–385.

Yoon, K., and K. J. Marfurt, 2006, Reverse-time migration using the pointing vector: Exploration Geophysics, **37**, 102–107.

Yoon, K., C. Shin, S. Suh, and L. R. Lines, 2003, 3D reverse-time migration using the acoustic wave equation: An experience with the SEG/EAGE data set: The Leading Edge, **22**, 38–41.